

# Few-Photon Single-Atom Cavity QED With Input-Output Formalism in Fock Space

Eden Rephaeli and Shanhui Fan, *Fellow, IEEE*

(Invited Paper)

**Abstract**—The Jaynes–Cummings (JC) system, which describes the interaction between a cavity and a two-level atom, is one of the most important systems in quantum optics. We obtain analytic solutions for the one- and two-photon transport in a waveguide side-coupled to the JC system using input–output formalism in Fock space. With these results, we discuss the conditions under which the JC system functions as a photon switch for waveguide photons in both the strong and weak coupling regimes.

**Index Terms**—Atom optics, cavity resonators, microwave photonics, nanophotonics, optical switches, optical waveguide, quantum dots, resonance light scattering.

## I. INTRODUCTION

CONTROLLABLE interaction between light and matter at the few-photon level is one of the main pursuits in quantum information processing [1]. Much attention has been focused on quantum two-level systems in the form of atoms [2] and quantum dots [3]–[5] in the optical frequency range, or Rydberg atoms [6], and superconducting Josephson junctions [7]–[9] in the microwave frequency range. All of these different forms of quantum two-level systems can be described by the same model; in this paper, we refer to them simply as “two-level atom.” The two-level atom is often placed in a cavity, which may enhance or inhibit spontaneous emission [10]. In the strong-coupling regime, the atom coherently exchanges energy with cavity photons [6], [11]–[15], as observed in vacuum Rabi-splitting [16] of the out-coupled photon spectra [4], [17]

We consider a system consisting of a waveguide side-coupled to a single-mode cavity containing a two-level atom. An example of such system is shown in Fig. 1(a) for the case where both the waveguide and the cavity are in a photonic crystal. This geometry has been demonstrated in several recent experiments [8], [18]–[22]. Theoretically, the atom-cavity system has been extensively studied with both numerical and analytic techniques. Numerically, this system has been simulated with an inherently stochastic quantum trajectory method [23]–[25], and by directly solving the Master equation with a truncated number-state basis describing the photons in the cavity [18], [26]–[28]. Analytically, this system can be analyzed with a coherent-state input by solving the time evolution of the density ma-

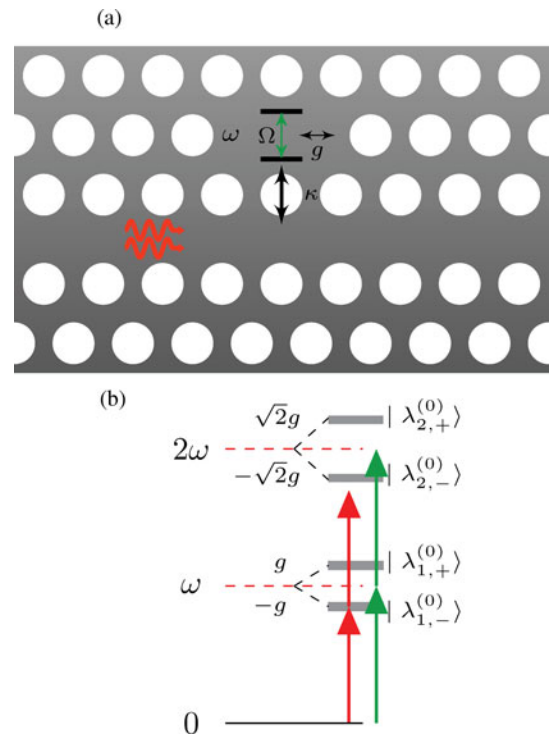


Fig. 1. (a) Schematic of a two-level atom in a cavity side coupled to a waveguide. (b) Energy spectrum of the JC hamiltonian ( $\Omega = \omega$ ) in the excitation number manifolds  $n = 0, 1$ , and  $2$ . Arrows show one and two photon absorption for two-photon switch. The switch is observed in reflection in the strong-coupling regime (red arrows), and in transmission in the weak-coupling regime (green arrows).

trix [29]–[31], or by using input–output formalism assuming with the weak-excitation approximation [2], [32].

We provide a fully quantum mechanical study of one- and two-photon waveguide transport through the atom-cavity system. Previously, single-photon transport was studied by solving for the real-space representation of the one-excitation eigenstate of the system [33], [34], while two-photon transport was studied using the field theoretic LSZ formalism [15]; both of these solutions are exact. Here, we rederive the one- and two-photon S-matrices using input–output formalism [35] in Fock space [36]. Our analytic results are in complete agreement with [15] and [33].

While the analytic results we present in this paper are known in the literature, we believe our rederivation is of significance. First of all, in comparison with the real-space wavefunction, and the LSZ field theoretic approach, input–output formalism is

Manuscript received December 31, 2011; revised April 11, 2012; accepted April 15, 2012.

The authors are with the Department of Applied Physics, Stanford University, Stanford, CA 94305 USA (e-mail: edenr@stanford.edu; shanhui@stanford.edu).

Color versions of one or more of the figures in this paper are available online at <http://ieeexplore.ieee.org>.

Digital Object Identifier 10.1109/JSTQE.2012.2196261

more widely used in quantum optics. Traditional use of input–output formalism, however, has largely focused on solving for properties of quantum systems with a coherent or squeezed state input. In this regard, it is of value to demonstrate how one can use the same formalism to solve for transport properties of Fock states in a geometry that is of direct experimental importance. Second, in the case of two-photon transport, input–output formalism in fact results in a much simpler and far more transparent derivation of the two-photon scattering matrix, compared with the LSZ technique. Third, our Fock-state approach may be generalized for more than two incident photons, and also multiple atoms [37], thus complimenting approaches with similar capabilities that are based on coherent-state excitations [38]–[41]. We, therefore, believe our work here can facilitate greater understanding of the transport properties of nonclassical Fock states in this experimentally important geometry.

In [28] and [42], it was theoretically and experimentally demonstrated that the unequal energy level spacing in the JC ladder, shown in Fig. 1(b), gives rise to photon-blockade, where a single-photon blocks the transport of a second, identical photon, through a direct-coupled cavity. This effect is analogous to the Coulomb blockade effect in condensed matter physics, where one electron blocks the transmission of a second electron through sufficiently small semiconductor islands due to the single-electron charging energy [43]. Using our analytic results, we show that when the cavity is side coupled, the system can act as a two-photon switch in both the strong and weak coupling regimes, and discuss the connection to photon blockade in the direct-coupled cavity.

The structure of this paper is as follows. In Section II, the Hamiltonian of the system is introduced, and equations of motion are derived. In Section III, the single-photon S-matrix is calculated, and single-photon transport is discussed. In Section IV, the two-photon S-matrix and the response to a two-photon plane wave are calculated. In Section V, we discuss the two-photon switch behavior.

## II. HAMILTONIAN AND EQUATIONS OF MOTION

A cavity containing a single two-level atom is described by the Jaynes–Cummings (JC) hamiltonian [44]:

$$H_{JC} = \frac{1}{2}\Omega\sigma_z + \omega c^\dagger c + g [c^\dagger\sigma_- + \sigma_+c] \quad (1)$$

where  $\Omega$  is the atomic transition frequency,  $\omega$  is the cavity mode frequency, and  $g$  is the atom-cavity coupling rate. The atom and cavity operators satisfy  $[\sigma_+, \sigma_-] = \sigma_z$  and  $[c, c^\dagger] = 1$ , respectively. We side-couple the atom-containing cavity described by (1) to a waveguide with linear dispersion relation and group velocity  $v_g$  for right- and left-moving photons [see Fig. 1(a)], with respective real-space photon creation (annihilation) operators  $a_R^\dagger(x)[a_R(x)]$  and  $a_L^\dagger(x)[a_L(x)]$ , satisfying  $[a_R(x), a_R^\dagger(x')] = [a_L(x), a_L^\dagger(x')] = \delta(x - x')$ . We refer to this atom-cavity-waveguide system as the *two-mode model*. To solve the two-mode model, we exploit the spatial inversion symmetry of the system by decomposing the Hilbert Space into even and odd subspaces with respective photon opera-

tors  $a_e(x) \equiv \frac{1}{\sqrt{2}}[a_R(x) + a_L(-x)]$  and  $a_o(x) \equiv \frac{1}{\sqrt{2}}[a_R(x) - a_L(-x)]$ , satisfying  $[a_e(x), a_e^\dagger(x')] = [a_o(x), a_o^\dagger(x')] = \delta(x - x')$ . Both even and odd subspaces feature a one-way (chiral) waveguide mode, but only the waveguide mode in the even subspace couples to the JC system. We refer to the system in the even subspace as the *one-mode model*. We will solve for the S-matrix of the one-mode model, from which the two-mode model S-matrix is then straightforwardly constructed (see [36, Appendix A]). The one-mode model hamiltonian is given by

$$H_e = v_g \int dk k a_k^\dagger a_k + V \int dk [a_k^\dagger c + c^\dagger a_k] + H_{JC} \quad (2)$$

where  $V$  is the waveguide-cavity coupling strength. The waveguide photon operator  $a_k = \frac{1}{\sqrt{2\pi}} \int dx e^{ikx} a_e(x)$  satisfies  $[a_k, a_{k'}^\dagger] = \delta(k - k')$ , where we omitted the  $e$  subscript from the  $k$ -space photon operators. Throughout this paper, we set  $v_g = 1$ .

Heisenberg operator equations for  $a_k(t)$ ,  $\sigma_-(t)$  and  $c(t)$  follow from (2):

$$\frac{da_k(t)}{dt} = -ika_k(t) - iVc(t) \quad (3)$$

$$\frac{dc(t)}{dt} = -i\omega c(t) - iV \int dk a_k(t) - ig\sigma_-(t) \quad (4)$$

$$\frac{d\sigma_-(t)}{dt} = -i\Omega\sigma_-(t) + ig\sigma_z(t)c(t). \quad (5)$$

In Appendix A, we follow the approach of [36], defining input and output waveguide photon operators, leading to

$$a_{\text{out}}(t) = a_{\text{in}}(t) - i\sqrt{\kappa} c(t) \quad (6)$$

$$\frac{dc(t)}{dt} = \left(-i\omega - \frac{\kappa}{2}\right) c(t) - i\sqrt{\kappa} a_{\text{in}}(t) - ig\sigma_-(t). \quad (7)$$

where  $\kappa \equiv 2\pi V^2$ . Equations (5)–(7) are the fundamental equations in the input–output formalism for this system. Here, we will solve these equations for one and two-photon scattering matrix (S-matrix).

## III. ONE-PHOTON SCATTERING MATRIX

The single-photon S-matrix between two free single-photon states with initial and final energies  $k$  and  $p$ , respectively, may be expressed using input and output operators as [36]

$${}_e\langle p|\mathbf{S}|k\rangle_e = \langle p^- | k^+ \rangle = \langle 0|a_{\text{out}}(p)a_{\text{in}}^\dagger(k)|0\rangle. \quad (8)$$

Here,  $|k^+\rangle$  and  $|p^-\rangle$  are scattering eigenstates that evolve in the interaction picture from free-photon states in the distant past and future, respectively [36]. Making use of

$$a_{\text{out}}(k) = a_{\text{in}}(k) - i\sqrt{\kappa} c(k) \quad (9)$$

the Fourier transform of (6), we rewrite (8) using input-field operators:

$$\langle p^- | k^+ \rangle = \delta(k - p) - i\sqrt{\kappa}\langle 0|c(p)|k^+\rangle.$$

To calculate the matrix element  $\langle 0 | c(p) | k^+ \rangle$ , we derive an equation of motion for its time-domain counterpart  $\langle 0|c(t)|k^+\rangle$

using (7), resulting in

$$\frac{d}{dt}\langle 0|c(t)|k^+\rangle = \left(-i\omega - \frac{\kappa}{2}\right)\langle 0|c(t)|k^+\rangle - i\sqrt{\kappa}\langle 0|a_{\text{in}}(t)|k^+\rangle - ig\langle 0|\sigma_-(t)|k^+\rangle \quad (10)$$

where  $\langle 0|a_{\text{in}}(t)|k^+\rangle = \frac{1}{\sqrt{2\pi}}e^{-ikt}$ , and from (5)  $\langle 0|\sigma_-(t)|k^+\rangle$  satisfies

$$\frac{d}{dt}\langle 0|\sigma_-(t)|k^+\rangle = -i\Omega\langle 0|\sigma_-(t)|k^+\rangle - ig\langle 0|c(t)|k^+\rangle. \quad (11)$$

Here, we have used the fact that  $\sigma_z|0\rangle = -|0\rangle$ . Equation (11) can be obtained alternatively using the weak excitation approximation by setting  $\sigma_z \rightarrow -1$  in (5). Thus, the weak excitation approximation is in fact justified when treating single-photon transport. However, in the single-photon calculation, the approach here can also be used to directly calculate the excitation of the atom.

The solutions to (10) and (11) yield:

$$\begin{aligned} \langle 0|c(p)|k^+\rangle &= \frac{\sqrt{\kappa}(k-\Omega)}{(k-\omega+i\frac{\kappa}{2})(k-\Omega)-g^2}\delta(k-p) \\ &\equiv s_k^{(c)}\delta(k-p) \end{aligned}$$

$$\begin{aligned} \langle 0|\sigma_-(p)|k^+\rangle &= \frac{\sqrt{\kappa}g}{(k-\omega+i\frac{\kappa}{2})(k-\Omega)-g^2}\delta(k-p) \\ &\equiv s_k^{(a)}\delta(k-p) \end{aligned}$$

$$\begin{aligned} \langle p^-|k^+\rangle &= \frac{(k-\omega-i\frac{\kappa}{2})(k-\Omega)-g^2}{(k-\omega+i\frac{\kappa}{2})(k-\Omega)-g^2}\delta(k-p) \\ &\equiv t_k\delta(k-p) \end{aligned}$$

where  $s^{(c)}(k)$ ,  $s^{(a)}(k)$ , and  $t_k$  are the cavity and atom excitation amplitudes, and the one-mode transmission coefficient, respectively. We note that the poles of all three functions are  $\lambda_{1,\pm} = \frac{\omega+\Omega-i\frac{\kappa}{2}}{2} \pm \sqrt{(\frac{\omega-\Omega-i\frac{\kappa}{2}}{2})^2 + g^2}$ . In the limit  $\kappa \rightarrow 0$ , we have  $\lambda_{1,\pm}$  approaching the one-excitation eigenvalues  $\lambda_{1,\pm}^{(0)}$  of the JC Hamiltonian.

Having derived the scattering matrix for the aforementioned one-mode model, we can straightforwardly obtain the transmission and reflection amplitudes for the two-mode model:

$$\begin{aligned} {}_R\langle p|\mathbf{S}|k\rangle_R &= \bar{t}_k\delta(k-p) \\ {}_L\langle p|\mathbf{S}|k\rangle_R &= \bar{r}_k\delta(k+p) \end{aligned}$$

where  $\bar{t}_k = \frac{1}{2}(t_k + 1)$ ,  $\bar{r}_k = \frac{1}{2}(t_k - 1)$ , and  $|k\rangle_{R,L} = \frac{1}{\sqrt{2\pi}}\int dx e^{ikx} a_{R,L}^\dagger(x)|0\rangle$ . In the following, we provide a brief discussion of the properties of the single-photon transport for the two-mode model, while only highlighting those aspects that are relevant for the discussions of the two-photon properties. A detailed discussion of single-photon transport in this system can be found in [33].

In Fig. 2, the transmission spectrum for the case of atom and cavity on-resonance ( $\omega = \Omega$ ) is plotted. We plot both the weak coupling regime with  $g < \kappa$  [see Fig. 2(a)], and the strong coupling regime with  $g > \kappa$  [see Fig. 2(b)]. In both regimes, three extrema are present in the spectrum. Two transmission

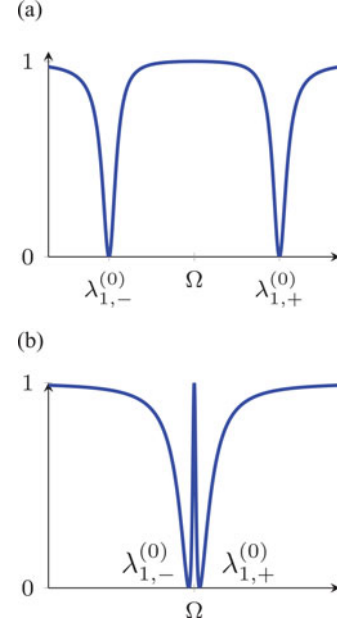


Fig. 2. Single-photon transmission  $|\bar{t}_k|^2$  versus incoming photon angular frequency in the case of tuned atom and cavity ( $\omega = \Omega$ ). (a) Strong-coupling regime ( $g > \kappa$ ). (b) Weak-coupling regime ( $g < \kappa$ ).

minima where the incident photon is completely reflected occur at  $k = \lambda_{1,\pm}^{(0)} = \omega \pm g$ , the single-excitation energy eigenvalue of the JC hamiltonian. At these frequencies,  $s_{k=\lambda_{1,\pm}^{(0)}}^{(c)} = \pm s_{k=\lambda_{1,\pm}^{(0)}}^{(a)}$ , the cavity and atom excitations have equal amplitudes and either equal or opposite phase. The transmission spectra have a maximum at  $k = \Omega$ , where the incident photon is fully transmitted. At this frequency, the cavity excitation amplitude is zero ( $s_{k=\Omega}^{(c)} = 0$ ), while the atomic excitation amplitude is maximal  $s_{k=\Omega}^{(a)} = -\sqrt{\kappa}/g$ . This is the dipole-induced transparency effect pointed out in [32]. In the strong coupling regime [see Fig. 2(a)], the spectral width of each transmission dip is  $\kappa/2$ , independent of the value of  $g$ , while in the weak-coupling regime the transmission spectrum displays the electromagnetically induced transparency type of feature, with a narrow central transmission peak whose width is proportional to  $g$ , as shown in Fig. 2(b).

#### IV. TWO-PHOTON SCATTERING MATRIX

In the one-mode model, the two-photon S-matrix  ${}_{ee}\langle p_1, p_2|\mathbf{S}_{ee}|k_1, k_2\rangle_{ee} = \langle p_1 p_2^-|k_1 k_2^+\rangle$ , connecting an incoming two-photon state with photon energies  $k_1$  and  $k_2$  to an outgoing two-photon state with photon energies  $p_1$  and  $p_2$ , may be written as [36] follows:

$$\begin{aligned} &\langle 0|a_{\text{out}}(p_2)a_{\text{out}}(p_1)a_{\text{in}}^\dagger(k_2)a_{\text{in}}^\dagger(k_1)|0\rangle \\ &= \int dp \langle p_1^-|p^+\rangle \langle p^+|a_{\text{out}}(p_2)a_{\text{in}}^\dagger(k_2)a_{\text{in}}^\dagger(k_1)|0\rangle \\ &= t_{p_1} \langle p_1^+|a_{\text{out}}(p_2)a_{\text{in}}^\dagger(k_2)a_{\text{in}}^\dagger(k_1)|0\rangle \end{aligned}$$

where we have inserted a complete single-photon basis above, and made use of the one-photon S-matrix from Section III.

Substituting (9), we obtain

$$\langle p_1 p_2^- | k_1 k_2^+ \rangle = t_{p_1} \langle p_1^+ | a_{\text{in}}(p_2) | k_1 k_2^+ \rangle - i\sqrt{\kappa} \langle p_1^+ | c(p_2) | k_1 k_2^+ \rangle.$$

In order to calculate  $\langle p_1^+ | c(p_2) | k_1 k_2^+ \rangle$ , we obtain a differential equations for its time-domain counterpart  $\langle p_1^+ | c(t) | k_1 k_2^+ \rangle$  using (4):

$$\begin{aligned} \frac{d}{dt} \langle p_1^+ | c(t) | k_1 k_2^+ \rangle &= -i \left( \omega - i \frac{\kappa}{2} \right) \langle p_1^+ | c(t) | k_1 k_2^+ \rangle \\ &\quad - i\sqrt{\kappa} \langle p_1^+ | a_{\text{in}}(t) | k_1 k_2^+ \rangle - ig \langle p_1^+ | \sigma_-(t) | k_1 k_2^+ \rangle \end{aligned} \quad (12)$$

where  $\langle p_1^+ | \sigma_-(t) | k_1 k_2^+ \rangle$  satisfies

$$\begin{aligned} \frac{d}{dt} \langle p_1^+ | \sigma_-(t) | k_1 k_2^+ \rangle &= -i\Omega \langle p_1^+ | \sigma_-(t) | k_1 k_2^+ \rangle \\ &\quad + ig \langle p_1^+ | \sigma_z(t) c(t) | k_1 k_2^+ \rangle \end{aligned} \quad (13)$$

as can be obtained using (5). We must now solve for the matrix element  $\langle p_1^+ | \sigma_z(t) c(t) | k_1 k_2^+ \rangle$  in (13), which may be rewritten using the identity  $\sigma_z = 2\sigma_+ \sigma_- - 1$  as follows:

$$\begin{aligned} \langle p_1^+ | \sigma_z(t) c(t) | k_1 k_2^+ \rangle &= 2 \langle p_1^+ | \sigma_+(t) | 0 \rangle \langle 0 | \sigma_-(t) c(t) | k_1 k_2^+ \rangle \\ &\quad - \langle p_1^+ | c(t) | k_1 k_2^+ \rangle. \end{aligned} \quad (14)$$

Examining (14), we note that the weak-excitation approximation ( $\sigma_z \rightarrow -1$ ) certainly does not hold. The first term on the right-hand side of (14), which would be completely absent in the weak-excitation limit, is in fact responsible for two-photon resonances in the S-matrix. To proceed, we generate an equation for the matrix element  $\langle 0 | \sigma_-(t) c(t) | k_1 k_2^+ \rangle$

$$\begin{aligned} \frac{d}{dt} \langle 0 | \sigma_-(t) c(t) | k_1 k_2^+ \rangle &= -i \left( \omega + \Omega - i \frac{\kappa}{2} \right) \langle 0 | \sigma_-(t) c(t) | k_1 k_2^+ \rangle \\ &\quad - i\sqrt{\kappa} \langle 0 | \sigma_-(t) a_{\text{in}}(t) | k_1 k_2^+ \rangle - ig \langle 0 | c^2(t) | k_1 k_2^+ \rangle \end{aligned} \quad (15)$$

where  $\langle 0 | c^2(t) | k_1 k_2^+ \rangle$  satisfies

$$\begin{aligned} \frac{d}{dt} \langle 0 | c^2(t) | k_1 k_2^+ \rangle &= -2i \left( \omega - i \frac{\kappa}{2} \right) \langle 0 | c^2(t) | k_1 k_2^+ \rangle \\ &\quad - 2i\sqrt{\kappa} \langle 0 | c(t) a_{\text{in}}(t) | k_1 k_2^+ \rangle - 2ig \langle 0 | \sigma_-(t) c(t) | k_1 k_2^+ \rangle. \end{aligned} \quad (16)$$

In deriving (16) we have used the identity  $[c(t), a_{\text{in}}(t)] = 0$  (see [37, Appendix A] for a similar proof). We now have a closed set of ordinary differential equations for the various matrix elements involved. Equations (15) and (16) may then be solved for  $\langle 0 | \sigma_-(t) c(t) | k_1 k_2^+ \rangle$ . Using this solution, we solve (12) and (13), and obtain the two-photon S-matrix:

$$\begin{aligned} \langle p_1 p_2^- | k_1 k_2^+ \rangle &= t_{p_1} t_{p_2} [\delta(k_1 - p_1) \delta(k_2 - p_2) \\ &\quad + \delta(k_1 - p_2) \delta(k_2 - p_1)] + B \delta(E_o - E_i) \end{aligned} \quad (17)$$

where

$$\begin{aligned} B &= \frac{i\sqrt{\kappa}g}{\pi} s_{p_1}^{(a)} s_{p_2}^{(a)} \\ &\quad \times \frac{2g [s_{k_1}^{(c)} + s_{k_2}^{(c)}] + (E_i - 2\omega + i\kappa) [s_{k_1}^{(a)} + s_{k_2}^{(a)}]}{(E_i - \lambda_{2,+})(E_i - \lambda_{2,-})} \end{aligned}$$

is the fluorescent term—the source of photon correlation effects, and  $E_i = k_1 + k_2$ ,  $E_o = p_1 + p_2$  are the total energy

of the incident and outgoing photons, respectively. The aforementioned S-matrix is identical to  $S_{p_1 p_2 k_1 k_2}$  in [15, eq. (6)], which was obtained using the field-theoretic LSZ method. The present derivation is more elementary. Also, in the present derivation, the S-matrix's composition in terms of one-photon excitation amplitudes and the role of the two-photon poles,

$\lambda_{2,\pm} = \frac{\Omega + 3\omega - i\frac{3\kappa}{2}}{2} \pm \sqrt{\left(\frac{\Omega - \omega + i\frac{\kappa}{2}}{2}\right)^2 + 2g^2}$ , is transparent.

Starting from the S-matrix for the one-mode model in (17), we obtain the scattering amplitudes in the two-mode model between planewave states corresponding to right- and left-propagating photons following the procedure in [11]:

$$\begin{aligned} {}_{RR} \langle p_1 p_2 | S | k_1 k_2 \rangle_{RR} &= \bar{t}_{k_1} \bar{t}_{k_2} [\delta(k_1 - p_1) \delta(k_2 - p_2) \\ &\quad + \delta(k_1 - p_2) \delta(k_2 - p_1)] + \frac{1}{4} B \delta(E_i - E_o) \\ {}_{LL} \langle p_1 p_2 | S | k_1 k_2 \rangle_{RR} &= \bar{r}_{k_1} \bar{r}_{k_2} [\delta(k_1 + p_1) \delta(k_2 + p_2) \\ &\quad + \delta(k_1 + p_2) \delta(k_2 + p_1)] + \frac{1}{4} B \delta(E_i - E_o) \\ {}_{RL} \langle p_1 p_2 | S | k_1 k_2 \rangle_{RR} &= \bar{t}_{k_1} \bar{r}_{k_2} [\delta(k_1 - p_1) \delta(k_2 + p_2) \\ &\quad + \delta(k_1 - p_2) \delta(k_2 + p_1)] + \frac{1}{4} B \delta(E_i - E_o). \end{aligned}$$

We consider an incident two-photon planewave state  $|k_1 k_2\rangle_{RR}$ , comprised of two right-going photons with individual energies  $k_1$  and  $k_2$ , as described by

$$|k_1 k_2\rangle_{RR} = \int dx_1 dx_2 S_{k_1, k_2}(x_1, x_2) \frac{1}{\sqrt{2}} a_R^\dagger(x_1) a_R^\dagger(x_2) |0\rangle$$

where  $S_{k_1, k_2}(x_1, x_2) = \frac{1}{\sqrt{2}2\pi} [e^{ik_1 x_1} e^{ik_2 x_2} + e^{ik_1 x_2} e^{ik_2 x_1}]$  is a symmetrized two-photon planewave. The resulting outgoing state  $|\phi\rangle$ , calculated in Appendix B, consists of three two-photon states

$$|\phi\rangle = |\phi\rangle_{RR} + |\phi\rangle_{LL} + |\phi\rangle_{RL}$$

describing two right-moving, two-left moving, and a right and left moving photons, respectively, given by

$$\begin{aligned} |\phi\rangle_{RR} &= \int dx_1 dx_2 \left\{ \bar{t}_{k_1} \bar{t}_{k_2} S_{k_1, k_2}(x_1, x_2) + H(x_1, x_2) \right\} \times \\ &\quad \frac{1}{\sqrt{2}} a_R^\dagger(x_1) a_R^\dagger(x_2) |0\rangle \end{aligned} \quad (18)$$

$$\begin{aligned} |\phi\rangle_{LL} &= \int dx_1 dx_2 \left\{ \bar{r}_{k_1} \bar{r}_{k_2} S_{k_1, k_2}(-x_1, -x_2) + H(-x_1, -x_2) \right\} \times \\ &\quad \frac{1}{\sqrt{2}} a_L^\dagger(x_1) a_L^\dagger(x_2) |0\rangle \end{aligned} \quad (19)$$

$$\begin{aligned} |\phi\rangle_{RL} &= \int dx_1 dx_2 \left\{ \frac{1}{2\pi} e^{iE_i x/2} [\bar{t}_{k_1} \bar{r}_{k_2} e^{2i\Delta_i x} + \bar{t}_{k_2} \bar{r}_{k_1} e^{-2i\Delta_i x}] \right. \\ &\quad \left. + \sqrt{2} H(x_1, -x_2) \right\} a_R^\dagger(x_1) a_L^\dagger(x_2) |0\rangle \end{aligned} \quad (20)$$



where

$$H(x_1, x_2) \equiv \frac{ig^2\kappa}{4\sqrt{2}} \frac{F(k_1, k_2)e^{iE_i x_c}}{(\lambda_{1,+} - \lambda_{1,-})(E_i - \lambda_{1,-} - \lambda_{1,+})} \\ \times \left[ \frac{e^{i(E_i - 2\lambda_{1,-})|x|/2}}{(E_i - 2\lambda_{1,-})} - \frac{e^{i(E_i - 2\lambda_{1,+})|x|/2}}{(E_i - 2\lambda_{1,+})} \right].$$

Above, we have defined the two-photon center-of-mass  $x_c \equiv \frac{x_1 + x_2}{2}$ , and spatial separation  $x \equiv x_1 - x_2$  coordinates; we also define  $\Delta_i = \frac{k_1 - k_2}{2}$ ,  $\Delta_o = \frac{p_1 - p_2}{2}$  and

$$F(k_1, k_2) \\ \equiv i \frac{\sqrt{\kappa}g}{\pi} \frac{2g \left[ s_{k_1}^{(c)} + s_{k_2}^{(c)} \right] + (E_i - 2\omega + i\kappa) \left[ s_{k_1}^{(a)} + s_{k_2}^{(a)} \right]}{(E_i - \lambda_{2,+})(E_i - \lambda_{2,-})}. \quad (21)$$

Photon statistics of the transmitted and reflected two-photon states is studied through the second-order coherence function  $g^{(2)}(\tau) = G^{(2)}(\tau)/|G^{(1)}(0)|^2$ , where  $G^{(1)}(\tau) = {}_{FF} \langle \phi | a_F^\dagger(y + \tau) a_F(y) | \phi \rangle_{FF}$ ,  $G^{(2)}(\tau) = {}_{FF} \langle \phi | a_F^\dagger(y) a_F^\dagger(y + \tau) a_F(y + \tau) a_F(y) | \phi \rangle_{FF}$ , and  $F = R, L$ . Here, we calculate  $g^{(2)}$  using the expression  $g^{(2)}(\tau) = G^{(2)}(\tau)/G^{(2)}(\tau \rightarrow \infty)$ , which is a consequence of  $\lim_{\tau \rightarrow \infty} g^{(2)}(\tau) = 1$ .  $g^{(2)}(\tau)$  is accessible experimentally through two-photon coincidence counting. With the help of  $g^{(2)}(\tau)$ , we now discuss how the JC system can function as a two-photon switch.

## V. TWO-PHOTON SWITCH

Based on the analytic results presented earlier, we provide a discussion of two scenarios where the system can behave as a two-photon switch, for energy degenerate photons. Our discussion of the strong-coupling regime mirrors that of [15]. As a point of departure, here, we also discuss a photon-switch in the weak-coupling regime, thus providing a unified discussion of both regimes.

### A. Strong-Coupling Regime

The two-photon switch in the strong-coupling regime is a consequence of the anharmonicity of the JC ladder [28]. As discussed in Section III, one incident photon tuned to the single-excitation eigenstate of the JC system,  $k = \lambda_{1,\pm}^{(0)}$ , is fully reflected. However, the energy of two such incident photons  $E_i = 2k = 2\lambda_{1,\pm}^{(0)}$ , does not coincide with a two-excitation eigenstate of the JC system, as illustrated by red arrows in Fig. 1(b). Consequently, the two photons are prevented from simultaneously entering the cavity. Since reflection in the side-coupled cavity considered here arises entirely from cavity field decay, subpoissonian statistics  $g^{(2)}(0) \ll 1$  is observed for the two reflected photons, as shown in Fig. 3(a). Additionally,  $g^{(2)}(\tau)$  of the two reflected photons exhibits strong antibunching and subpoissonian statistics for all time intervals  $\tau$ , as shown in Fig. 3(b). Here, a sufficiently large coupling rate  $g$  is needed to ensure that the two-photon energy does not overlap with the two-excitation energy eigenstates, which are broadened due to waveguide coupling. We note that the photon switch behavior

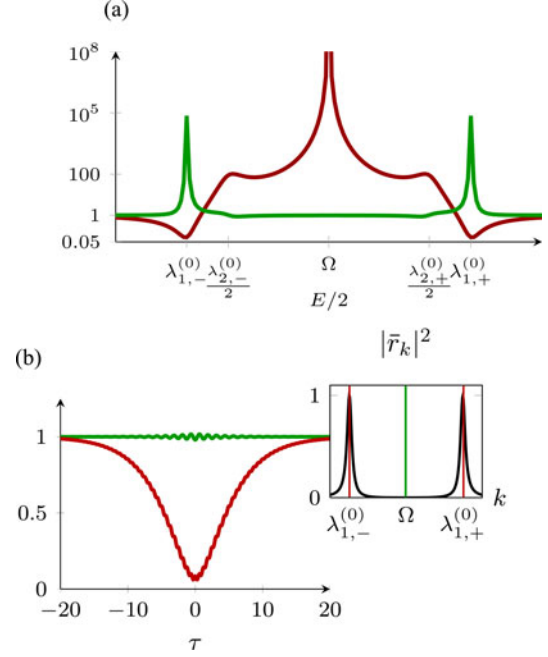


Fig. 3. Strong coupling regime ( $g = \sqrt{5}\kappa$ ). (a) Reflected  $g^{(2)}(0)$  versus  $E/2$  in red curve; Transmitted  $g^{(2)}(0)$  versus  $E/2$  in green curve. (b) Reflected two-photon  $g^{(2)}(\tau)$  for  $E/2 = \lambda_{1,\pm}^{(0)}$  in red curve; transmitted two-photon  $g^{(2)}(\tau)$  for  $E/2 = \Omega$  is green curve. Inset: Single-photon reflection spectrum  $|r_k|^2$ .

in reflection described above in the side-coupled cavity is identical to the photon-blockade reported in transmission through a direct-coupled cavity [28], [42].

In addition to the photon switching behavior in reflection for  $E_i/2 = \lambda_{1,\pm}^{(0)}$ , the  $g^{(2)}(0)$  spectrum also exhibits other interesting features. In reflection,  $g^{(2)}(0)$  peaks at  $E_i/2 = \Omega$ , exhibiting superpoissonian statistics [see Fig. 1(a)]. This behavior is attributed to the vanishing single-photon reflection at  $k = \Omega$ , since  $g^{(2)}(\tau)$  is normalized with respect to  $G^{(1)}(0)$ , which vanishes when single-photon reflection vanishes. We note that in the direct-coupled cavity system, the superpoissonian statistics shown here in two-photon reflection at  $E_i/2 = \Omega$  occurs in transmission instead [42], [45], and is named “photon-induced tunneling” [42]. In transmission,  $g^{(2)}(0)$  peaks at  $E_i/2 = \lambda_{1,\pm}^{(0)}$ , displaying superpoissonian statistics [see Fig. 1(a)], which is attributed to the vanishing single-photon transmission at  $k_1 = \lambda_{1,\pm}^{(0)}$ . Finally, in transmission,  $g^{(2)}(0) \approx 1$  for all time intervals  $\tau$  at  $E_i/2 = \Omega$ . At this frequency, the atom excitation scales as  $1/g$ , and is, therefore, weakly excited under strong coupling, resulting in poissonian statistics for the transmitted light [see Fig. 1(a)].

### B. Weak-Coupling Regime

A two-photon switch in the weak-coupling regime is also possible in this system, without requiring a nonlinear cavity [46]. Here, the photon switch is created due to the intrinsic nonlinearity of the atom [47], [48]. As discussed in Section III,

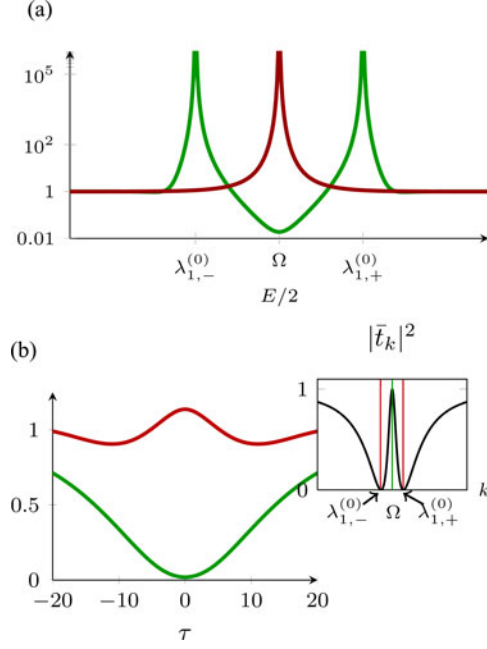


Fig. 4. Weak coupling regime ( $g = \frac{\kappa}{\sqrt{5}}$ ). (a) Reflected  $g^{(2)}(0)$  versus  $E/2$  in red curve; Transmitted  $g^{(2)}(0)$  versus  $E/2$  in green curve. (b) Reflected two-photon  $g^{(2)}(\tau)$  for  $E/2 = \lambda_{1,s}^{(0)}$  in red curve; transmitted two-photon  $g^{(2)}(\tau)$  for  $E/2 = \Omega$  is green curve. Inset: Single-photon transmission.

one incident photon tuned to  $k = \Omega$ , is completely transmitted. However, when two such photons, each with an energy  $E_i/2 = \Omega$ , are incident, subpoissonian statistics  $g^{(2)}(0) \ll 1$  is observed for the two transmitted photons, as shown in Fig. 4(a).  $g^{(2)}(\tau)$  of the two transmitted photons is antibunched, and displays subpoissonian statistics for all time intervals  $\tau$ , as shown in Fig. 4(b). Thus, the presence of the atom in the cavity results in complete single-photon transmission (dipole-induced transparency), but the inability of the atom to absorb more than one photon at a time leads to antibunching and subpoissonian statistics in two-photon transmission. We note that a similar atom-induced photon switch occurs when the atom is directly coupled to a waveguide [11]. There, a single photon is completely reflected, whereas antibunching is observed in two-photon reflection  $g^{(2)}(0) = 0$ ,

Furthermore, the two-photon reflection at  $E_i/2 = \Omega$  displays superpoissonian statistics as a result of the vanishing single-photon reflection at  $k = \Omega$ . Finally, as is the case of strong coupling, superpoissonian statistics is observed in two-photon transmission at  $E_i/2 = \lambda_{1,\pm}^{(0)}$ .

## VI. FINAL REMARK AND CONCLUSION

As a final remark, we note that in practice, in addition to coupling to the cavity which is in turn coupled to the waveguide, the atom also couples to nonguided modes, leading to loss. This loss may be accounted for by making the replacement  $\Omega \rightarrow \Omega - i\gamma/2$  where  $\gamma$  is the coupling rate into nonguided modes [49]. For the case of the D2 transition of a Caesium atom placed in a Fabry–Perot cavity, this loss can be on the order of the cavity linewidth [28]. In contrast, for the case of a

self-assembled InAs quantum dot in a photonic crystal cavity, the atom loss is roughly two orders of magnitude smaller than the cavity linewidth [42], and, therefore, does not lead to a qualitative difference in the transport properties with respect to the nonlossy case. Here, we, therefore, ignore the effects of atomic loss.

In conclusion, we have solved for the one- and two-photon S-matrices in a waveguide side-coupled to a cavity containing a two-level atom. Our solution is based on input–output formalism [35], in the Fock space [36], and is fully quantum-mechanical and deterministic. We have discussed the features of one-photon transport, and the photon-switch effect in both the weak- and strong-coupling regime, as seen in the transport of a two-photon planewave state. Using the S-matrices presented in this paper, the response to one and two incident waveguide photons with arbitrary spectra and pulse shapes may be straightforwardly obtained.

## APPENDIX A

### DERIVATION OF INPUT–OUTPUT RELATIONS FOR WAVEGUIDE PHOTON OPERATORS

Following the approach of [36], we integrate (3) from time  $t_0 \rightarrow -\infty$  to obtain

$$a_k(t) = e^{-ik(t-t_0)} a_k(t_0) - iV \int_{t_0}^t dt' c(t') e^{-ik(t-t')}. \quad (22)$$

We define  $\kappa \equiv 2\pi V^2$ , the waveguide-cavity coupling rate. Additionally, we define the operator  $\Phi(t) \equiv \frac{1}{\sqrt{2\pi}} \int dk a_k(t)$ , the input-field operator  $a_{\text{in}}(t) \equiv \frac{1}{\sqrt{2\pi}} \int dk e^{-ik(t-t_0)} a_k(t_0)$ , and sum (A) over  $k$ , leading to

$$\Phi(t) = a_{\text{in}}(t) - i\sqrt{\frac{\kappa}{4}} c(t). \quad (23)$$

We also define an output field operator  $a_{\text{out}}(t) \equiv \frac{1}{\sqrt{2\pi}} \int dk e^{-ik(t-t_1)} a_k(t_1)$ , integrate (3) from time  $t_1 \rightarrow \infty$ , and sum over  $k$ , leading to

$$\Phi(t) = a_{\text{out}}(t) + i\sqrt{\frac{\kappa}{4}} c(t). \quad (24)$$

Equating (23) and (24) we obtain

$$a_{\text{out}}(t) = a_{\text{in}}(t) - i\sqrt{\kappa} c(t).$$

Plugging (24) into (4), we obtain

$$\frac{dc}{dt} = -i \left( \omega - i\frac{\kappa}{2} \right) c(t) - i\sqrt{\kappa} a_{\text{in}}(t) - ig\sigma_-(t).$$

We have, thus, obtained the input–output formalism [see (6) and (7)] for this system.

## APPENDIX B

## TWO-PHOTON PLANEWAVE TRANSPORT

Consider an incident two-photon planewave state with right-moving photons:

$$|k_1, k_2\rangle_{RR} = \int dx_1 dx_2 S_{k_1, k_2}(x_1, x_2) \frac{1}{\sqrt{2}} a_R^\dagger(x_1) a_R^\dagger(x_2) |0\rangle \quad (25)$$

where  $S_{k_1, k_2}(x_1, x_2) = \frac{1}{\sqrt{22\pi}} [e^{ik_1 x_1} e^{ik_2 x_2} + e^{ik_1 x_2} e^{ik_2 x_1}]$ . We decompose the state in (25) into even and odd subspaces by noting that

$$\begin{aligned} |x_1, x_2\rangle_{RR} &= \frac{1}{\sqrt{2}} a_R^\dagger(x_1) a_R^\dagger(x_2) |0\rangle \\ &= \frac{1}{\sqrt{2}} \frac{1}{\sqrt{2}} [a_e^\dagger(x_1) + a_o^\dagger(x_1)] \frac{1}{\sqrt{2}} [c_e^\dagger(x_2) + c_o^\dagger(x_2)] |0\rangle \\ &= \frac{1}{2\sqrt{2}} a_e^\dagger(x_1) a_e^\dagger(x_2) |0\rangle + \frac{1}{2\sqrt{2}} a_o^\dagger(x_1) a_o^\dagger(x_2) |0\rangle \\ &\quad + \frac{1}{2\sqrt{2}} a_e^\dagger(x_1) a_o^\dagger(x_2) |0\rangle + \frac{1}{2\sqrt{2}} a_o^\dagger(x_1) a_e^\dagger(x_2) |0\rangle \\ &= \frac{1}{2} |x_1, x_2\rangle_{ee} + \frac{1}{2} |x_1, x_2\rangle_{oo} + \frac{1}{2\sqrt{2}} |x_1, x_2\rangle_{eo} \\ &\quad + \frac{1}{2\sqrt{2}} |x_1, x_2\rangle_{oe}. \end{aligned}$$

It follows that

$$\begin{aligned} |k_1, k_2\rangle_{RR} &= \frac{1}{2} |k_1, k_2\rangle_{ee} + \frac{1}{2} |k_1, k_2\rangle_{ee} \\ &\quad + \frac{1}{2\sqrt{2}} |k_1, k_2\rangle_{eo} + \frac{1}{2\sqrt{2}} |k_1, k_2\rangle_{oe} \end{aligned}$$

where  $|k_1, k_2\rangle_{ee} = \int dx_1 dx_2 S_{k_1, k_2}(x_1, x_2) \frac{1}{\sqrt{2}} a_e^\dagger(x_1) a_e^\dagger(x_2) |0\rangle$  and for e.g.  $|k_1, k_2\rangle_{eo} = \int dx_1 dx_2 S_{k_1, k_2}(x_1, x_2) a_e^\dagger(x_1) a_o^\dagger(x_2) |0\rangle$ . We can now apply the scattering operator:

$$\begin{aligned} \mathbf{S}|k_1, k_2\rangle_{RR} &= \frac{1}{2} \mathbf{S}_{ee} |k_1, k_2\rangle_{ee} + \frac{1}{2} \mathbf{S}_{oo} |k_1, k_2\rangle_{oo} \\ &\quad + \frac{1}{2\sqrt{2}} \mathbf{S}_{eo} |k_1, k_2\rangle_{eo} + \frac{1}{2\sqrt{2}} \mathbf{S}_{oe} |k_1, k_2\rangle_{oe} \end{aligned} \quad (26)$$

where  $\mathbf{S}|k_1, k_2\rangle_{RR}$  is the out-state (scattered state). In the following, we work through each one of the terms in (26).

A. *eo* and *oe* Subspaces

In the *eo* subspace the scattering operator is  $\mathbf{S}_{eo} = \mathbf{S}_e \mathbf{S}_o = \mathbf{S}_e \mathbf{I}_o$ , where  $\mathbf{I}_o$  is the identity operator in the odd subspace. We may then rewrite the third term in (26)

$$\begin{aligned} \frac{1}{2\sqrt{2}} \mathbf{S}_e \mathbf{I}_o |k_1, k_2\rangle_{eo} &= \\ &= \frac{1}{2\sqrt{2}} \int dx_1 dx_2 \frac{1}{\sqrt{22\pi}} [e^{ik_1 x_1} e^{ik_2 x_2} + e^{ik_1 x_2} e^{ik_2 x_1}] \\ &\quad \times \mathbf{S}_e a_e^\dagger(x_1) a_o^\dagger(x_2) |0\rangle. \end{aligned}$$

Inserting a one-photon resolution of the identity twice, we rewrite as follows:

$$\begin{aligned} &= \frac{1}{2\sqrt{2}} \int dx_1 dx_2 \frac{1}{\sqrt{22\pi}} [e^{ik_1 x_1} e^{ik_2 x_2} + e^{ik_1 x_2} e^{ik_2 x_1}] \\ &\quad \times \int dk \int dp |p\rangle_e \langle p| \mathbf{S}_e |k\rangle_e \langle k| x_1\rangle_e |x_2\rangle_o \end{aligned}$$

noting that  $\langle p| \mathbf{S}_e |k\rangle_e = t_k \delta(k - p)$  we have

$$\begin{aligned} &\frac{1}{2\sqrt{2}} \mathbf{S}_e \mathbf{I} |k_1, k_2\rangle_{eo} \\ &= \frac{1}{2\sqrt{2}} \int dx_1 dx_2 \frac{1}{\sqrt{22\pi}} [t_{k_1} e^{ik_1 x_1} e^{ik_2 x_2} + t_{k_2} e^{ik_1 x_2} e^{ik_2 x_1}] \\ &\quad \times a_e^\dagger(x_1) a_o^\dagger(x_2) |0\rangle. \end{aligned}$$

Similarly, in the *oe* subspace we have:

$$\begin{aligned} &\frac{1}{2\sqrt{2}} \mathbf{S}_e \hat{\mathbf{I}} |k_1, k_2\rangle_{oe} = \\ &= \frac{1}{2\sqrt{2}} \int dx_1 dx_2 \frac{1}{\sqrt{22\pi}} [t_{k_2} e^{ik_1 x_1} e^{ik_2 x_2} + t_{k_1} e^{ik_1 x_2} e^{ik_2 x_1}] \\ &\quad \times a_o^\dagger(x_1) a_e^\dagger(x_2) |0\rangle \end{aligned}$$

B. *oo* Subspace

In the *oo* subspace the scattering operator is  $\mathbf{S}_{oo} = \mathbf{S}_o \mathbf{S}_o = \mathbf{I}_o \mathbf{I}_o$  where  $\mathbf{I}_o$  is the identity operator in the odd subspace. Applying the scattering operator we have

$$\frac{1}{2} \mathbf{S}_o \mathbf{S}_o |k_1, k_2\rangle_{oo} = \frac{1}{2} |k_1, k_2\rangle_{oo}$$

C. *ee* Subspace

In the *ee* subspace we have

$$\begin{aligned} &\frac{1}{2} \mathbf{S}_{ee} |k_1, k_2\rangle_{ee} \\ &= \frac{1}{2} \int_{-\infty}^{\infty} dp_1 \int_{-\infty}^{p_1} dp_2 |p_1, p_2\rangle_{ee} \langle p_1, p_2| \mathbf{S}_{ee} |k_1, k_2\rangle_{ee} \end{aligned}$$

where we have inserted a two-photon resolution of the identity. We use the result in (17)

$$\begin{aligned} &\frac{1}{2} \mathbf{S}_{ee} |k_1, k_2\rangle_{ee} \\ &= \frac{1}{2} \int dp_1 \int dp_2 \left\{ t_{k_1} t_{k_2} \right. \\ &\quad \times \left[ \delta(k_1 - p_1) \delta(k_2 - p_2) + \delta(k_1 - p_2) \delta(k_2 - p_1) \right] \\ &\quad \left. + s_{p_1}^{(a)} s_{p_2}^{(a)} F(k_1, k_2) \delta(k_1 + k_2 - p_1 - p_2) \right\} \times |p_1, p_2\rangle_{ee} \end{aligned} \quad (27)$$

where  $|p_1, p_2\rangle_{ee} = \frac{\sqrt{2}}{2\pi} \int dx_1 dx_2 e^{iE_o x_c} \cos \Delta_o x |x_1, x_2\rangle_{ee}$ , and  $F(k_1, k_2)$  was defined in (2). The first term in (27)—the

uncorrelated transport term—is equal to  $\frac{1}{2}t_{k_1}t_{k_2}|k_1, k_2\rangle_{ee}$ . The second term is equal to

$$\frac{\sqrt{2}}{4\pi}F(k_1, k_2) \int dx_1 dx_2 |x_1, x_2\rangle_{ee} \int_{-\infty}^{\infty} dE_o e^{iE_o x_c} \delta(E_i - E_o) \int_{-\infty}^0 d\Delta_o \cos[\Delta_o x] s_{p_1}^{(a)} s_{p_2}^{(a)}.$$

Integrating over  $E_o$  and exploiting the invariance of the integrand under the inversion  $\Delta_o \rightarrow -\Delta_o$ :

$$= \frac{\sqrt{2}}{8\pi}F(k_1, k_2) \int dx_1 dx_2 e^{iE_i x_c} |x_1, x_2\rangle_{ee} \int_{-\infty}^{\infty} d\Delta_o e^{i\Delta_o x} s_{p_1}^{(a)} s_{p_2}^{(a)}$$

or

$$= \frac{\sqrt{2}g^2\kappa}{8\pi}F(k_1, k_2) \int dx_1 dx_2 e^{iE_i x_c} |x_1, x_2\rangle_{ee} \int_{-\infty}^{\infty} \frac{d\Delta_o e^{i\Delta_o x}}{(\Delta_o + E_i/2 - \lambda_{1,-})(\Delta_o + E_i/2 - \lambda_{1,+})} \times \frac{1}{(\Delta_o - E_i/2 + \lambda_{1,-})(\Delta_o - E_i/2 + \lambda_{1,+})}.$$

Integrating over  $\Delta_o$  using the residue theorem:

$$= \frac{ig^2\kappa}{2\sqrt{2}}F(k_1, k_2) \int dx_1 dx_2 e^{iE_i x_c} \times \left\{ \frac{e^{i(E_i/2 - \lambda_{1,-})|x|}}{(\lambda_{1,+} - \lambda_{1,-})(E_i - 2\lambda_{1,-})(E_i - \lambda_{1,-} - \lambda_{1,+})} + \frac{e^{i(E_i/2 - \lambda_{1,+})|x|}}{(\lambda_{1,-} - \lambda_{1,+})(E_i - 2\lambda_{1,+})(E_i - \lambda_{1,+} - \lambda_{1,-})} \right\} \times |x_1, x_2\rangle_{ee}.$$

Finally, we combine the uncorrelated and correlated terms and get

$$\frac{1}{2}\mathbf{S}_{ee}|k_1, k_2\rangle_{ee} = \frac{1}{2}t_{k_1}t_{k_2}|k_1, k_2\rangle_{ee} + \frac{ig^2\kappa}{2\sqrt{2}}F(k_1, k_2) \int dx_1 dx_2 e^{iE_i x_c} \times \left\{ \frac{e^{i(E_i/2 - \lambda_{1,-})|x|}}{(\lambda_{1,+} - \lambda_{1,-})(E_i - 2\lambda_{1,-})(E_i - \lambda_{1,-} - \lambda_{1,+})} + \frac{e^{i(E_i/2 - \lambda_{1,+})|x|}}{(\lambda_{1,-} - \lambda_{1,+})(E_i - 2\lambda_{1,+})(E_i - \lambda_{1,+} - \lambda_{1,-})} \right\} |x_1, x_2\rangle_{ee}.$$

We then add together the results of Appendixes B-A, B-B, and B-C, and use the definition  $a_e^\dagger = \frac{a_R^\dagger(x) + a_L^\dagger(-x)}{\sqrt{2}}$  and  $a_o^\dagger = \frac{a_R^\dagger(x) - a_L^\dagger(-x)}{\sqrt{2}}$  to express the out-state in terms of left and right moving photons, as presented in (18)–(20).

## REFERENCES

- [1] H. J. Kimble, “The quantum internet,” *Nature*, vol. 453, pp. 1023–1030, 2008.
- [2] R. J. Thompson, G. Rempe, and H. J. Kimble, “Observation of normal-mode splitting for an atom in an optical cavity,” *Phys. Rev. Lett.*, vol. 68, pp. 1132–1135, Feb. 1992.
- [3] T. Yoshie, A. Scherer, J. Hendrickson, G. Khitrova, H. M. Gibbs, G. Rupper, C. Ell, O. B. Shchekin, and D. G. Deppe, “Vacuum rabi splitting with a single quantum dot in a photonic crystal nanocavity,” *Nature*, vol. 432, pp. 200–203, 2004.
- [4] G. Khitrova, H. M. Gibbs, M. Kira, S. W. Koch, and A. Scherer, “Vacuum rabi splitting in semiconductors,” *Nat. Phys.*, vol. 2, no. 2, pp. 81–90, 2006.
- [5] D. Press, S. Götzinger, S. Reitzenstein, C. Hofmann, A. Löffler, M. Kamp, A. Forchel, and Y. Yamamoto, “Photon antibunching from a single quantum-dot-microcavity system in the strong coupling regime,” *Phys. Rev. Lett.*, vol. 98, p. 117402, Mar. 2007.
- [6] M. Brune, F. Schmidt-Kaler, A. Maali, J. Dreyer, E. Hagley, J. M. Raimond, and S. Haroche, “Quantum rabi oscillation: A direct test of field quantization in a cavity,” *Phys. Rev. Lett.*, vol. 76, no. 3, 1996.
- [7] Y. Nakamura, Y. A. Pashkin, and J. S. Tsai, “Coherent control of macroscopic quantum states in a single-cooper-pair box,” *Nature*, vol. 398, no. 4, pp. 786–788, 1999.
- [8] A. Wallraff, D. I. Schuster, A. Blais, L. Frunzio, R.-S. Huang, J. Majer, S. Kumar, S. M. Girvin, and R. J. Schoelkopf, “Strong coupling of a single photon to a superconducting qubit using circuit quantum electrodynamics,” *Nature*, vol. 431, pp. 162–167, Sep. 2004.
- [9] C. Lang, D. Bozyigit, C. Eichler, L. Steffen, J. M. Fink, A. A. Abdumalikov, M. Baur, S. Philipp, M. P. da Silva, A. Blais, and A. Wallraff, “Observation of resonant photon blockade at microwave frequencies using correlation function measurements,” *Phys. Rev. Lett.*, vol. 106, p. 243601, Jun. 2011.
- [10] D. Kleppner, “Inhibited spontaneous emission,” *Phys. Rev. Lett.*, vol. 47, pp. 233–236, Jul. 1981.
- [11] J. T. Shen and S. Fan, “Strongly correlated multiparticle transport in one dimension through a quantum impurity,” *Phys. Rev. A*, vol. 76, p. 062709, Dec. 2007.
- [12] M. Devoret, S. Girvin, and R. Schoelkopf, “Circuit-qed: How strong can the coupling between a josephson junction atom and a transmission line resonator be?,” *Ann. Phys.*, vol. 16, no. 10–11, pp. 767–779, 2007.
- [13] K. Srinivasan, O. Painter, “Mode coupling and cavity–quantum-dot interactions in a fiber-coupled microdisk cavity,” *Phys. Rev. A*, vol. 75, p. 023814, Feb. 2007.
- [14] E. Rephaeli, J. T. Shen, and S. Fan, “Full inversion of a two-level atom with a single-photon pulse in one-dimensional geometries,” *Phys. Rev. A*, vol. 82, p. 033804, Sep. 2010.
- [15] T. Shi, S. Fan, and C. P. Sun, “Two-photon transport in a waveguide coupled to a cavity in a two-level system,” *Phys. Rev. A*, vol. 84, p. 063803, Dec. 2011.
- [16] J. J. Sanchez-Mondragon, N. B. Narozhny, and J. H. Eberly, “Theory of spontaneous-emission line shape in an ideal cavity,” *Phys. Rev. Lett.*, vol. 51, pp. 550–553, Aug. 1983.
- [17] D. Englund, A. Majumdar, A. Faraon, M. Toishi, N. Stoltz, P. Petroff, and J. Vučković, “Resonant excitation of a quantum dot strongly coupled to a photonic crystal nanocavity,” *Phys. Rev. Lett.*, vol. 104, p. 073904, Feb. 2010.
- [18] K. Srinivasan and O. Painter, “Linear and nonlinear optical spectroscopy of a strongly coupled microdisk-quantum dot system,” *Nature*, vol. 450, no. 12, pp. 862–865, 2007.
- [19] B. Dayan, A. S. Parkins, T. Aoki, E. P. Ostby, K. J. Vahala, and H. J. Kimble, “A photon turnstile dynamically regulated by one atom,” *Science*, vol. 319, no. 5866, pp. 1062–1065, 2008.
- [20] J. M. Fink, M. Goppl, M. Baur, R. Bianchetti, P. J. Leek, A. Blais, and A. Wallraff, “Climbing the jaynes-cummings ladder and observing its nonlinearity in a cavity qed system,” *Nature*, vol. 454, no. 7, pp. 315–318, 2008.
- [21] R. J. Schoelkopf and S. M. Girvin, “Wiring up quantum systems,” *Nature*, vol. 451, pp. 664–669, Feb. 2008.
- [22] A. Faraon, I. Fushman, D. Englund, N. Stoltz, P. Petroff, and J. Vuckovic, “Dipole induced transparency in waveguide coupled photonic crystal cavities,” *Opt. Express.*, vol. 16, pp. 12154–12162, Aug. 2008.
- [23] J. Dalibard, Y. Castin, and K. Mølmer, “Wave-function approach to dissipative processes in quantum optics,” *Phys. Rev. Lett.*, vol. 68, pp. 580–583, Feb. 1992.



- [24] L. Tian and H. J. Carmichael, "Quantum trajectory simulations of two-state behavior in an optical cavity containing one atom," *Phys. Rev. A*, vol. 46, pp. R6801–R6804, Dec. 1992.
- [25] A. Faraon, A. Majumdar, and J. Vučković, "Generation of nonclassical states of light via photon blockade in optical nanocavities," *Phys. Rev. A*, vol. 81, p. 033838, Mar. 2010.
- [26] R. J. Brecha, P. R. Rice, and M. Xiao, "N two-level atoms in a driven optical cavity: Quantum dynamics of forward photon scattering for weak incident fields," *Phys. Rev. A*, vol. 59, pp. 2392–2417, Mar. 1999.
- [27] A. Blais, R.-S. Huang, A. Wallraff, S. M. Girvin, and R. J. Schoelkopf, "Cavity quantum electrodynamics for superconducting electrical circuits: An architecture for quantum computation," *Phys. Rev. A*, vol. 69, p. 062320, Jun. 2004.
- [28] K. M. Birnbaum, A. Boca, R. Miller, A. D. Boozer, T. E. Northup, and H. J. Kimble, "Photon blockade in an optical cavity with one trapped atom," *Nature*, vol. 436, no. 7, pp. 87–90, 2005.
- [29] G. S. Agarwal, "Vacuum-field rabi splittings in microwave absorption by rydberg atoms in a cavity," *Phys. Rev. Lett.*, vol. 53, pp. 1732–1734, Oct. 1984.
- [30] G. S. Agarwal and R. R. Puri, "Exact quantum-electrodynamics results for scattering, emission, and absorption from a rydberg atom in a cavity with arbitrary  $Q$ ," *Phys. Rev. A*, vol. 33, pp. 1757–1764, Mar. 1986.
- [31] H. J. Carmichael, "Photon antibunching and squeezing for a single atom in a resonant cavity," *Phys. Rev. Lett.*, vol. 55, pp. 2790–2793, Dec. 1985.
- [32] E. Waks and J. Vuckovic, "Dipole induced transparency in drop-filter cavity-waveguide systems," *Phys. Rev. Lett.*, vol. 96, p. 153601, Apr. 2006.
- [33] J.-T. Shen and S. Fan, "Theory of single-photon transport in a single-mode waveguide. i. coupling to a cavity containing a two-level atom," *Phys. Rev. A*, vol. 79, no. 2, 2009.
- [34] P. Bermel, A. Rodriguez, S. G. Johnson, J. D. Joannopoulos, and M. Soljačić, "Single-photon all-optical switching using waveguide-cavity quantum electrodynamics," *Phys. Rev. A*, vol. 74, p. 043818, Oct. 2006.
- [35] C. W. Gardiner and M. J. Collett, "Input and output in damped quantum systems: Quantum stochastic differential equations and the master equation," *Phys. Rev. A*, vol. 31, pp. 3761–3774, Jun. 1985.
- [36] S. Fan, Ş. E. Kocabaş, and J.-T. Shen, "Input-output formalism for few-photon transport in one-dimensional nanophotonic waveguides coupled to a qubit," *Phys. Rev. A*, vol. 82, p. 063821, Dec. 2010.
- [37] E. Rephaeli, Ş. E. E. Kocabaş, and S. Fan, "Few-photon transport in a waveguide coupled to a pair of colocated two-level atoms," *Phys. Rev. A*, vol. 84, p. 063832, Dec. 2011.
- [38] K. Koshino, "Novel method for solving the quantum nonlinear dynamics of photons: Use of a classical input," *Phys. Rev. Lett.*, vol. 98, p. 223902, Jun. 2007.
- [39] K. Koshino, "Single-photon filtering by a cavity quantum electrodynamics system," *Phys. Rev. A*, vol. 77, p. 023805, Feb. 2008.
- [40] K. Koshino, "Multiphoton wave function after kerr interaction," *Phys. Rev. A*, vol. 78, p. 023820, Aug. 2008.
- [41] S. E. Kocabas, E. Rephaeli, and S. Fan, "Resonance fluorescence in a waveguide geometry," *Phys. Rev. A*, vol. 85, p. 023817, Feb. 2012.
- [42] A. Faraon, I. Fushman, D. Englund, N. Stoltz, P. Petroff, and J. Vuckovic, "Coherent generation of non-classical light on a chip via photon-induced tunnelling and blockade," *Nat. Phys.*, vol. 4, no. 11, pp. 859–863, 2008.
- [43] K. Likharev, "Single-electron devices and their applications," *Proc. IEEE*, vol. 87, pp. 606–632, Apr. 1999.
- [44] E. Jaynes and F. Cummings, "Comparison of quantum and semiclassical radiation theories with application to the beam maser," *Proc. IEEE*, vol. 51, pp. 89–109, Jan. 1963.
- [45] A. Kubanek, A. Ourjoumtsev, I. Schuster, M. Koch, P. W. H. Pinkse, K. Murr, and G. Rempe, "Two-photon gateway in one-atom cavity quantum electrodynamics," *Phys. Rev. Lett.*, vol. 101, p. 203602, Nov. 2008.
- [46] A. Imamoglu, H. Schmidt, G. Woods, and M. Deutsch, "Strongly interacting photons in a nonlinear cavity," *Phys. Rev. Lett.*, vol. 79, pp. 1467–1470, Aug. 1997.
- [47] T. Aoki, A. S. Parkins, D. J. Alton, C. A. Regal, B. Dayan, E. Ostby, K. J. Vahala, and H. J. Kimble, "Efficient routing of single photons by one atom and a microtoroidal cavity," *Phys. Rev. Lett.*, vol. 102, p. 083601, Feb. 2009.
- [48] S. Rosenblum, S. Parkins, and B. Dayan, "Photon routing in cavity qed: Beyond the fundamental limit of photon blockade," *Phys. Rev. A*, vol. 84, p. 033854, Sep. 2011.
- [49] E. Rephaeli and S. Fan, *To be published*.

**Eden Rephaeli** received the B.Sc. degree in physics and the B.Sc. degree in electrical engineering from Tel Aviv University, Ramat Aviv, Israel, in 2006. He is currently working toward the Ph.D. degree in applied physics at Stanford University, Stanford, CA.

His research interests include quantum optics and nanophotonics.

**Shanhui Fan** (M'05–SM'06–F'11) received the Ph.D. degree in 1997 in theoretical condensed matter physics from the Massachusetts Institute of Technology (MIT), Cambridge, MA.

He is currently an Associate Professor of electrical engineering at Stanford University, Stanford, CA. Previously, he was a Research Scientist at the Research Laboratory of Electronics at MIT. His research interests include computational and theoretical studies of solid state and photonic structures and devices, especially photonic crystals, plasmonics, and meta-materials. He has published 240 refereed journal articles, given more than 180 invited talks, and was granted 39 U.S. patents.

Dr. Fan is a Fellow of the American Physical Society, OSA, and SPIE. He received the National Science Foundation Career Award in 2002, the David and Lucile Packard Fellowship in Science and Engineering in 2003, the National Academy of Sciences Award for Initiative in Research in 2007, and the Adolph Lomb Medal from the OSA in 2007.